Measurement of Thin Film Isotropic and Anisotropic Thermal Conductivity Using 3ω and Thermoreflectance Imaging

K. Maize[1], Y. Ezzahri[1], X. Wang[1], S. Singer[2], A. Majumdar[2] and A. Shakouri[1]*
1Department of Electrical Engineering, University of California Santa Cruz
1156 High Street, Santa Cruz, California 95064-1077, USA
2 Department of Mechanical Engineering, University of California Berkeley
Etcheverry Hall, Mailstop 1740, University of California, Berkeley, CA 94720, USA
* ali@soe.ucsc.edu

Abstract

The 3ω method is a well established technique for measuring thermal conductivity of thin films and substrates. The method extracts thermal conductivity by measuring temperature response when current flows through a metal strip heater deposited on the material's surface. The metal strip is used both as heat source and temperature sensor. An important factor in the accuracy of 3ω measurements is that the current should be confined to the metal strip resistor and any leakage to the substrate will invalidate the results. This is because the heat source would no longer be localized on the surface and also because any Schottky behavior at metal/semiconductor interface will create nonlinearities that affect the 3ω signal substantially. These problems are especially important at high temperatures where thermionic emission of electrons through oxide insulation layer becomes important. In this paper we propose thermoreflectance imaging as an additional method to determine thermal conductivity of thin film materials. Because thermoreflectance measures temperatures optically, the method is less dependent on the electrical properties of the metal heater. Additionally, the temperature profile near the heat source can be used to ensure there is no defect in the thin film metal heater. Theory is presented demonstrating thermoreflectance can also be used to measure anisotropic in-plane and cross-plane thermal conductivity in thin films. Preliminary thermoreflectance measurements were analyzed at various locations on the surface of isotropic, InGaAs and anisotropic ScN/ZrN superlattice thin film 3ω test samples. Experimental results are in agreement with simulated temperature distributions.

Keywords

Thermal conductivity measurement, anisotropy, thin film, superlattice, 3ω method, Thermoreflectance imaging.

1. Introduction

The 3ω technique has become standard in measuring thin film thermal conductivity [1-4]. The method works by measuring heat diffusion into a material resulting from a sinusoidal heat source. Three-ω was motivated by a fundamental problem of DC thermal conductivity measurement at room temperature, in which a significant fraction of the heat that is intended to flow through the solid instead radiates out of the sample. Because the 3ω method is an AC technique, heat loss due to radiation is negligible at sufficient excitation frequency. The 3ω method has proven very versatile. It is capable of measuring thermal conductivity for samples of varying layer configuration and can also extract anisotropic thermal conductivities in materials with different cross-plane and in-plane thermal components [4].

We propose thermoreflectance imaging together with a localized heat source as alternate method for measuring thermal conductivity in thin films. Because the thermoreflectance method uses the same fundamental governing heat equations as the 3ω method, it offers similar application to measuring both multilayer and anisotropic thermal conductivity. Thermoreflectance offers several advantages over the 3ω method. Thermal images provide instant, detailed, two-dimensional thermal maps of both the heat source and surrounding thin film surface. Any nonuniformity in the heating element or other thermal anomalies are immediately evident in the thermal image. These nonuniform components may not be detectable from electrical measurements alone using the 3ω method. Another advantage of thermoreflectance is that measurement of anisotropic thermal conductivity can theoretically be performed using a single heat source. In comparison, 3ω methods for measuring anisotropy require depositing two heat sources of different widths [4] and there are limitations in the minimum film thickness that can be analyzed.

2. Theoretical background

2.1. Surface temperature profile for an isotropic thin film on a semi-infinite isotropic substrate

A schematic diagram of the first test structure used in this study is shown in figure 1. The sample, originally configured for 3ω measurement, is comprised of a two micron InGaAs thin film semiconductor on top of a thermally thick InP substrate. They are separated by a 100 nm InAlAs buffer layer. The metal heater strip is deposited on top of the structure and electrically isolated from the thin film by a 185 nm SiO_2 layer.

In both 3ω and thermoreflectance methods the heater is excited by an AC current of frequency ω. The 3ω method uses the average temperature across the width of the heater to extract the thermal conductivity of the underlying thin film. With the thermoreflectance technique, we instead examine the thin film surface temperature distribution along a line extending perpendicular to the heater's long axis.

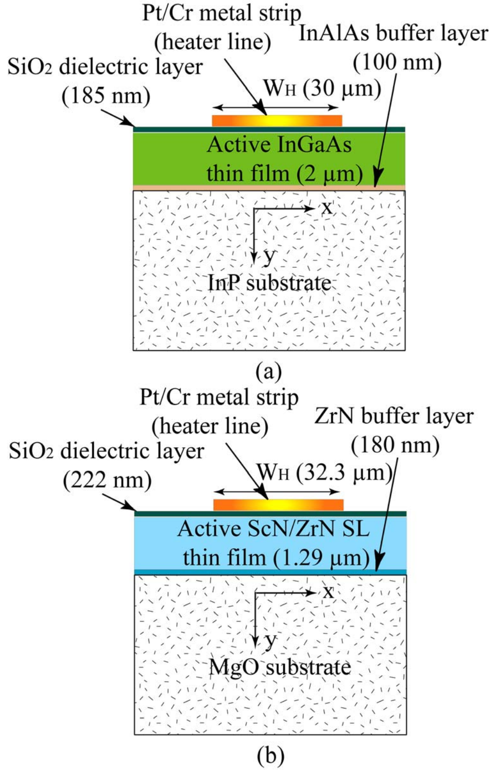

Figure 1: Schematic diagram of the two test structures studied; the isotropic InGaAs thin film on the isotropic InP substrate (a), and the anisotropic ScN/ZrN superlattice thin film on the isotropic MgO substrate (b).

The metal heater in the first sample is 30 µm wide, which is 15 times greater than the thickness of the top InGaAs semiconductor film. Additionally, the thermal conductivity of the top InGaAs film is expected to be much smaller than the thermal conductivity of InP. As discussed by many authors [1-6], under these conditions at low frequencies (<1kHz) the thin film can be modeled as thermal resistance. This resistance shifts the temperature distribution by a constant factor that is independent of the frequency of excitation of the heater, and given by:

$$\Delta T_f(x) = \Delta T_T(x) - \Delta T_S(x) = \frac{P}{l}\frac{d_f}{W_H \beta_f} \quad (1)$$

where $\Delta T_T(x)$, is the temperature distribution of the combined thin film and substrate, and $\Delta T_S(x)$ is the distribution of the substrate alone. P/l is the amplitude of the power per unit length generated at frequency 2ω in the heater. d_f and βf are the thickness and the thermal conductivity of the semiconductor thin film, respectively, and W_H is the width of the metal heater strip.

The characteristic length of temperature oscillations is given by the thermal penetration depth of the InP substrate q_S^{-1} defined by [1]:

$$q_S^{-1} = \sqrt{\frac{\alpha_S}{2i\omega}} \quad (2)$$

where α_S refers to the thermal diffusivity of the substrate. In the low frequency range (<1kHz) the thermal penetration depth of the InP substrate is very large compared to the metal heater strip width. Under these conditions the latter can be approximated as an infinitely narrow line.

The temperature oscillation at a distance x from an infinitely narrow line heat source on the surface of a semi-infinite substrate is given by [7]:

$$\Delta T_S(x) = \frac{P}{l\pi\beta_S} K_0(q_S x) \quad (3)$$

where K_0 is the zeroth-order modified Bessel function and β_S is the thermal conductivity of the substrate.

In figures 2 (a) and (b), we have plotted the modulus and phase of $\frac{\Delta T_T(x)}{P/l}$ as a function of distance from the line heat source for excitation frequencies f = 5, 30, and 106 Hz.

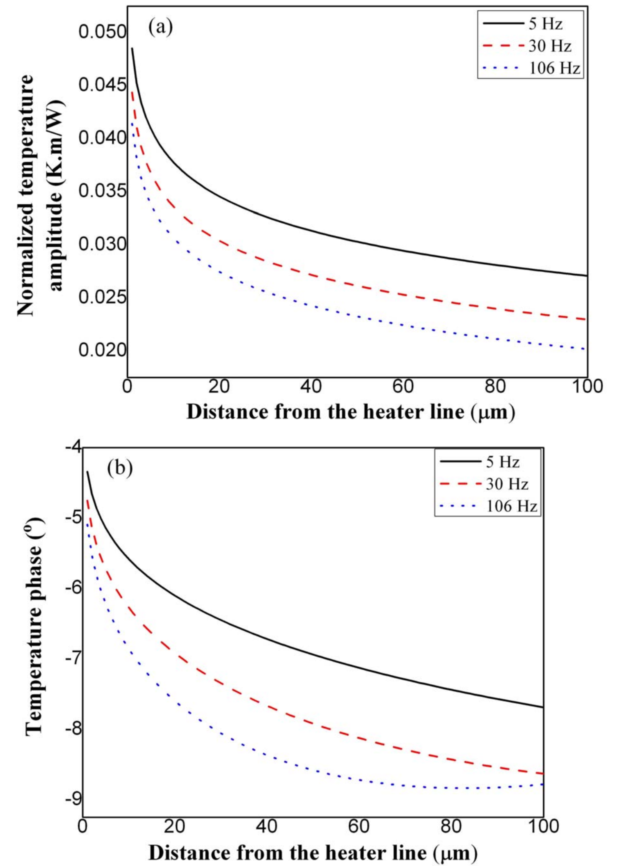

Figure 2: Simulated temperature amplitude (a) and phase (b) as a function of distance from the heater line for different frequencies, in the case of isotropic thin film on top of an isotropic InP semi-infinite substrate.

2.2. Application of thermoreflectance to extract thermal conductivity

With the temperature distributions provided by thermal images, thermal conductivity can be determined by comparing the ratio of temperatures for two points at known distances perpendicular to the heater. To demonstrate the concept, we consider two cases involving samples with isotropic thermal

conductivity. In the first, ideal, case we model the heat source as an infinitely narrow line on the surface of a semi-infinite substrate. In the second case we include the effect of a thin semiconductor film on top of a semi-infinite substrate and use a heater with a finite width W_H.

For both cases, we assume operation in the frequency range for which the thermal penetration depth q_S^{-1} is very large $q_S^{-1} >> W_H$, and we are interested in an area much smaller than a disc with radius q_S^{-1}.

In the first case the temperature distribution on the surface starting from the center of the heater line, is given by [1]:

$$\Delta T(x) = \frac{P}{l\pi\beta_S}\left\{\ln\left[\frac{2}{x}\sqrt{\frac{\alpha_S}{2\omega}}\right] - E_C - i\frac{\pi}{4}\right\} \quad (4)$$

where E_C=0.5772 is the Euler constant. If we take the ratio of the real part of equation (4) on two different points x_1 and x_2 at the vicinity of the metal heat line, we will have:

$$\frac{\mathrm{Re}[\Delta T(x_1)]}{\mathrm{Re}[\Delta T(x_2)]} = \frac{\mathrm{Re}\left[\frac{\Delta R}{R}(x_1)\right]}{\mathrm{Re}\left[\frac{\Delta R}{R}(x_2)\right]} = \frac{\ln\left[\frac{2}{x_1}\sqrt{\frac{\alpha_S}{2\omega}}\right] - E_C}{\ln\left[\frac{2}{x_2}\sqrt{\frac{\alpha_S}{2\omega}}\right] - E_C} = \varepsilon \quad (5)$$

After some algebra, it is very easy to get the expression for the thermal diffusivity of the substrate:

$$\alpha_S = \frac{\exp(2E_C)}{2}\omega\left(\frac{x_1}{x_2^{\varepsilon}}\right)^{\frac{2}{1-\varepsilon}} \quad (6)$$

Therefore the thermal properties of the film can be obtained from the real part of the thermoreflectance response at two locations on the film's surface. Note that because the power terms cancel, the calculation uses the thermoreflectance change on the surface and not the actual temperature. Therefore it is not necessary to calibrate for the thin film's thermoreflectance coefficient. In the second case, we assume a thin film on a substrate and we take into account the finite width of the heater line. By neglecting the thermal resistances at the different interfaces, the temperature distribution on the surface under the assumptions made above, is given by [2-4]:

$$\Delta T(x) = \frac{P}{l}\left\{\frac{1}{\pi\beta_S}\left[\ln\left(\frac{2}{x}\sqrt{\frac{\alpha_S}{2\omega}}\right) - E_C - i\frac{\pi}{4}\right] + \frac{d_f}{\beta_f W_H}\right\} \quad (7)$$

The same procedure as above plus some algebra allows us to get the expression of the thermal conductivity of the thin film as:

$$\beta_f^{-1} = \frac{W_H}{\pi\beta_S d_f}\left\{\ln\left[\sqrt{\frac{2\omega}{\alpha_S}}\left(\frac{x_1}{x_2^{\varepsilon}}\right)^{\frac{1}{1-\varepsilon}}\right] + E_C - \ln(2)\right\} \quad (8)$$

2.3. Measurement of the thermal conductivity anisotropy

Recently a very sophisticated analysis has been developed to improve the 3ω method to extract simultaneously the thermal conductivity, heat capacity, thermal conductivity anisotropy, and interlayer contact resistance in the general case of multilayer anisotropic structures [4, 5]. The two-dimensional analytical solution derived by Borca-Tasciuc et al [4] for the complex temperature distribution on the surface of multilayer structures with anisotropic thermophysical properties is one of the main results obtained to date using the 3ω technique.

Material anisotropy is especially sensitive to experimental conditions since it can only be detected by heat diffusion that is strongly two-dimensional. Figure 3 shows how the linewidth of the metal heater strip can influence the heat flow path [5].

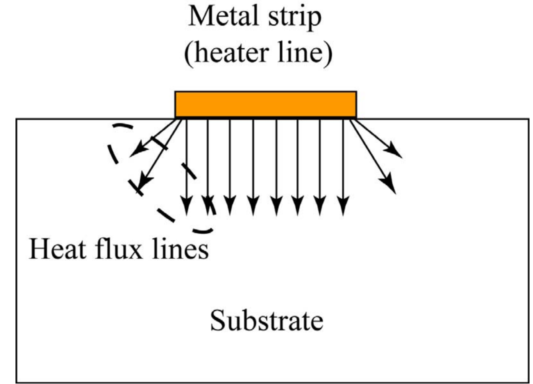

Figure 3: A sketch illustrating the effect of width of the metal heater strip on the heat flux path in a 3ω system.

In previous work, Borca-Tasciuc et al [4] used an iterative method using two metal heater strips of different widths deposited on the same sample to extract the thermal conductivity anisotropy of thin film nanochanneled alumina. Thermoreflectance imaging has the advantage of acquiring the temperature distribution over a large surface area including the metal heater strip and its vicinity in a single measurement. Starting from equation (1) of reference [4], we can show that the complex temperature distribution on the surface of a multilayer anisotropic structure would be given by:

$$\Delta T(x) = -\frac{P}{\pi l\beta_{y1}}\int_0^{\infty}\frac{\sin(kb)}{kb}\frac{\cos(kx)}{A_1 B_1}dk \quad (9)$$

where β_{y1} is the cross-plane thermal conductivity of the nominal thin film, A_1 and B_1 are as defined in reference [4], and b is the metal heater half-width $W_H/2$. The temperature distribution on the thin film very close to the heater edge would be sensitive to both the cross-plane and the in-plane components of its thermal conductivity. Using thermoreflectance imaging we can get the temperature profile at any frequency in the vicinity of the metal heater. Then, under the assumption of knowing the thermal properties of the substrate, it is easy to fit the experimental temperature profile using equation (9) and optimize the remaining free parameters to obtain the in-plane and cross-plane components of the thermal conductivity of the thin film.

As shown above, even in this general case, the thermoreflectance method does not need to know the amplitude of the power per unit length *(P/l)* in the heater. This term cancels when taking the ratio of temperatures in the vicinity of the metal heater.

3. Experiment

Figure 4 below shows a schematic diagram of the experimental set up used in the thermoreflectance imaging technique.

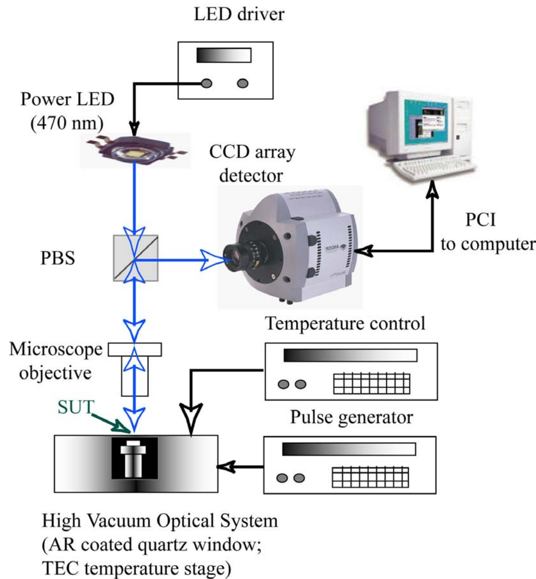

Figure 4: Schematic diagram of the experimental set-up used in the thermoreflectance imaging technique.

Thermoreflectance imaging is a proven and quick way to obtain temperature distributions on active device surfaces and interfaces. This optical, non-contact method can obtain two-dimensional thermal maps with submicron spatial resolution and 5-50 mK temperature resolution. This is accomplished by measuring the temperature dependent reflectivity change at the surface. References [8-19] provide a survey of thermoreflectance imaging techniques.

4. Results and discussion

Figure 5 (a) shows a thermoreflectance image of the heater line on top of the isotropic InGaAs thin film for an electrical excitation at 5 Hz. The relative change of reflectivity (R/R) decreases as a function of distance away from the heater line. Figures 5 (b) and (c) show the amplitude and phase profiles for the isotropic InGaAs sample obtained from thermoreflectance imaging at 5, 30, and 106 Hz. Profiles are taken along the perpendicular axis to the heater line as shown in figure 5 (a). In figure 5 (d) we have plotted together the smoothed experimental data at 5Hz and the simulated result based on the prediction of eq. 7, there is close agreement between the prediction and the experimentally obtained profiles.

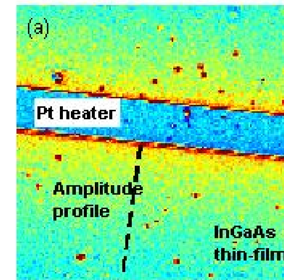

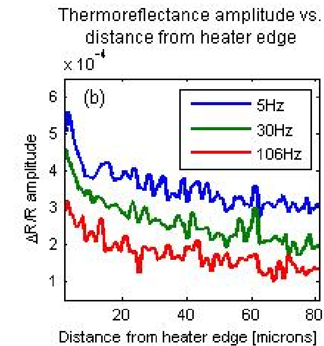

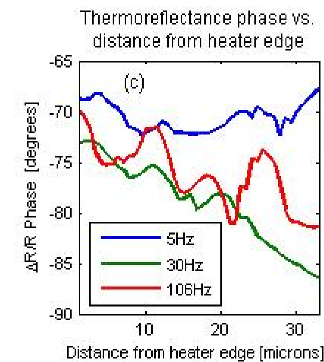

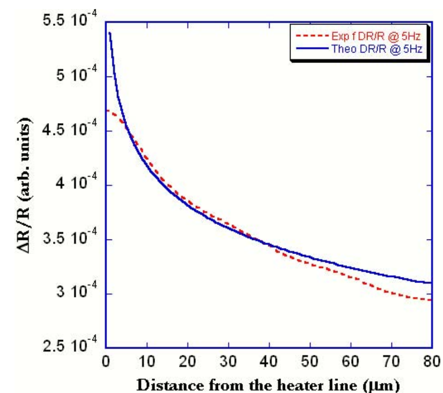

Figure 5: (a) Thermoreflectance image of the heater line on top of the InGaAs thin film sample. $\Delta R/R$ amplitude (b) and phase (c) profiles perpendicular to heater for frequencies 5, 30, and 106 Hz. (d) Smoothed $\Delta R/R$ amplitude profile at 5 Hz (dashed curve) and the corresponding fit (solid curve) based on eq. 7.

The active thin film in the second test structure we have studied is a 1.29 µm ScN/ZrN metal superlattice. The sample's MgO substrate is thermally thick and isotropic. The thin film is separated from the substrate by a 180 nm ZrN buffer layer. The metal heater strip is deposited on top of the structure and electrically isolated from the thin film superlattice by a 222 nm SiO_2 layer. A schematic diagram of the structure is illustrated in figure 1 (b). The artificial layered structure of the superlattice gives rise to anisotropic thermal properties.

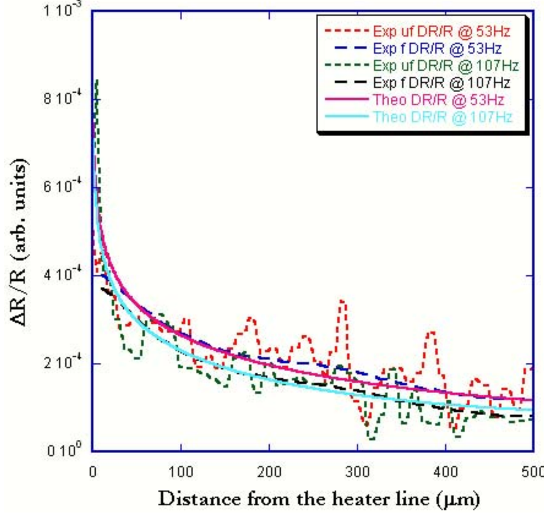

Figure 6: ΔR/R amplitude profiles perpendicular to the heater line on top of the anisotropic ScN/ZrN superlattice structure for frequencies 53, and 107 Hz

As we have shown in section 2, theoretically it is possible to extract both the in-plane and cross-plane components of the thermal conductivity of the thin film using the complete equation (9), or a simplified expression of this equation. The input experimental data would be two profiles of the real parts of ΔR/R for two different frequencies.

Figure 6 above shows the experimental amplitude of ΔR/R profiles as a function of distance from the heater line, for the case of the anisotropic ScN/ZrN superlattice on top of the isotropic semi-infinite MgO substrate. The figure shows the measurements for two modulation frequencies. The dotted curves represent the raw data, and the dashed curves represent the smoothed data after application of a linear filter to smooth the local fluctuation and to remove the noise. The solid lines represent the best fit for both frequencies with the same scaling factor to match the experimental ΔR/R data. The fit was obtained using an approximated expression of equation (9) given by:

$$\Delta T(x)=\frac{P}{l}\left\{\begin{array}{l}\frac{1}{\pi\beta_S}\left[\ln\left(\frac{2}{x}\sqrt{\frac{\alpha_S}{2\omega}}\right)-E_C-i\frac{\pi}{4}\right]\\+\frac{d_f}{W_H}\Phi\left(\beta_{Fx},\beta_{Fy}\right)\end{array}\right\} \quad (10)$$

where Φ is a function that describes the heat spreading into the thin superlattice film. Under some assumptions described in reference [4], this function could be simplified and given by:

$$\Phi\left(\beta_{Fx},\beta_{Fy}\right)=\frac{1}{\beta_{Fy}+0.76\frac{d_f}{W_H}\sqrt{\beta_{Fx}\beta_{Fy}}} \quad (11)$$

where β_{Fx} and β_{Fy} refer to the in-plane and cross-plane components of the thermal conductivity of the superlattice thin film, respectively. We have found that the fitting is more sensitive to the cross-plane component than to the in-plane one. $\beta_{Fy}=4.1$ W/m/K gives the best fit represented in figure 6. Since the results are less sensitive to β_{Fx}, we chose a value of β_{Fx} equal to 22 W/m/K, which is the bulk value of thermal conductivity for ZrN.

In fact, simulations have shown that the results would be more sensitive to the in-plane thermal conductivity and thereafter to the anisotropy of the thermal conductivity of the thin film if: (i) the heater line is very narrow, and/or (ii) the substrate thermal conductivity is equal to or less than the expected in-plane value of the thermal conductivity of the thin film. In other words, the ratio of the in-plane component of the thermal conductivity of the thin film to thermal conductivity of the substrate should be higher than 1 ($\beta_{Fx}/\beta_S>1$).

Unfortunately, none of the above conditions were fulfilled by the structure we have studied for the present sample. Nevertheless, the value of the cross-plane component of the thermal conductivity of the superlattice thin film that gives the best fitting is very close to the value extracted by 3ω method, which proves the thermoreflectance profiles to contain sufficient information to extract the thermal conductivity. The detailed application of thermoreflectance imaging to the extraction of the thermal conductivity anisotropy of thin films will be presented in a future work.

5. Conclusions

We have proposed thermoreflectance imaging as an alternate method to 3ω for extracting thermal conductivity in thin films and bulk materials. The method is valid for materials with either isotropic or anisotropic in-plane and cross-plane thermal conductivities. By working exclusively from the thermoreflectance distribution in the thermal image, the method is less sensitive to abnormalities in the electrical properties of the heat source than is the 3ω method. We have shown that calibration and absolute temperature values are not required in order to determine the thin film thermal conductivity.

Acknowledgments

The authors would like to thank Vijay Rawat and Prof. Tim Sands at Purdue and Dr. Joshua Zide and Prof. Art Gossard at UCSB for providing the material used in this

study. This work was funded in part by ONR MURI Thermionic Energy Conversion Center and by the SRC Interconnect Focus Center.

References

1. D. G. Cahill, Rev. Sci. Instrum, **61**, 802, (1990).
2. S. M. Lee and D. G. Cahill, J. Appl. Phys, 81, 2590, (1997).
3. J. H. Kim, A. Feldman, and D. Novotny, J. Appl. Phys, 86, 3959, (1999).
4. T. Borca-Tasciuc, A. R. Kumar, and G. Chen, 72, 2139, (2001).
5. B. W. Olson, S. Graham, and K. Chen, Rev. Sci. Instrum, 76, 053901, (2005).
6. T. Tong and A. Majumdar, Rev. Sci, Instrum, 77, 104902, (2006).
7. H. S. Carslaw and J. C. Jaeger, Conduction of Heat in Solids (Oxford University Press, Oxford, 1959).
8. S. Dilhaire, S. Grauby, and W. Cleays, Appl. Phys. Lett, 84, 822, (2004).
9. M. G. Burzo, P.L. Komarov, P.E. Raad, Components and Packaging Technologies, IEEE Transactions on, vol.28, no.4, pp. 637-643, Dec. 2005.
10. G. Tessier, S. Pavageau, B. Charlot, C. Filloy, D. Fournier, B. Cretin, S. Dilhaire, S. Gomes, N. Trannoy, P. Vairac, S. Volz, Components and Packaging Technologies, IEEE Transactions on, vol.30, no.4, pp.604-608, Dec. 2007.
11. J. Christofferson and A. Shakouri, Rev. Sci Instrum, 76, 024903, (2005).
12. J. Christofferson, D. Vashae, A. Shakouri, P. Melese, X. Fan; G. Zeng; C. Labounty, J.E. Bowers, E. T. Croke, Seventeenth Annual IEEE Semiconductor Thermal measurement and Management Symposium, San Jose, CA, USA, 20-22 March (2001).
13. J. Christofferson, D. Vashae, A. Shakouri, P. Melese, Proceedings of the SPIE, vol. 4275, San Jose, CA, USA, p.24-25 Jan. 2001 p.119-25.
14. G. Kaytaz, P. L. Komarov, and P. E. Raad, in Proc. 9th Int. IEEE Workshop THERMal INvestigations IC Systems (THERMINIC'03), Aix-en-Provence, France, Sep. 24–26, 2003, pp. 251–256.
15. K. E. Goodson, Y. S. Ju, Trans. of the ASME, p.306-313, May 1998.
16. V. Quintard, S. Dilhaire, T. Phan, W. Claeys, IEEE Transactions on Instrumentation and Measurement. Vol. 48, no. 1, pp. 69-74. Feb. 1999.
17. S. Grauby, B. C. Forget, S. Hole, and D. Fournier, Rev. Sci. Instrum. 70, 3603 (1999).
18. Y. S. Ju, K. E. Goodson, Journal of heat transfer, vol. 120, no2, pp. 306-313, 1998.
19. Z. Bian, J. Christofferson, A. Shakouri, P. Kozodoy, Appl. Phys. Lett., vol. 83, no. 17 pp. 3605-3607, 2003.